CHIN. PHYS. LETT. Vol. 34, No. 10 (2017) 104201

# Multi-Channel NRZ/RZ-DPSK to CSRZ-DPSK Format Conversion Based on Nonlinear Polarization Rotation of SOA *

Ya-Ya Mao(毛雅亚)[1]**, Chong-Qing Wu(吴重庆)[2], Xin-Zhi Sheng(盛新志)[2], Bo Liu(刘博)[1], Rahat Ullah[1], Feng Tian(田凤)[1]

[1]*Institute of Optoelectronics, Nanjing University of Information Science & Technology, Nanjing 210044*
[2]*Key Lab of Luminescence and Optical Information Technology (Ministry of Education), School of Science, Beijing Jiaotong University, Beijing 100044*

(Received 22 May 2017)

*We present an all-optical nonreturn-to-zero/return-to-zero (NRZ/RZ) to carrier-suppressed return-to-zero (CSRZ) format conversion scheme for differential phase-shift keying (DPSK) signals. The conversion is based on nonlinear polarization rotation of a semiconductor optical amplifier (SOA). The 4-channel NRZ-DPSK or RZ-DPSK signals at 10 Gb/s are simultaneously converted to the corresponding CSRZ-DPSK signals, with −0.8 and 1.4 dB average power penalties, respectively. Additionally, high quality format conversion performances are shown with the optical spectra and eye diagrams.*

*PACS:* 42.79.Sz, 42.25.Kb, 42.65.Yj, 42.65.Re DOI: 10.1088/0256-307X/34/10/104201

All-optical format conversion is a key function in providing flexible management and interface for different networks.[1,2] Previously, many studies proposed and demonstrated format conversions for the on-off keying (OOK) signals.[3−7] Recently, differential phase-shift keying (DPSK) signals have been widely used in long haul optical transmission systems, due to their lower optical signal-to-noise ratio requirements and higher tolerance to nonlinear effects.[8,9] It is therefore desirable to explore all optical format converters for such signals. Several all-optical format conversion schemes between nonreturn-to-zero (NRZ)-DPSK and return-to-zero (RZ)-DPSK signals have already been proposed and experimentally demonstrated.[10−12] Owing to their superior tolerance to nonlinear and dispersion impairments higher than that of many conventional RZ and NRZ modulation formats, the carrier-suppressed return-to-zero (CSRZ) modulation format, which reduces the main carrier component is widely used in high-spectral-efficiency wavelength division multiplexing (WDM) and dense WDM (DWDM) systems.[13,14] Thus all-optical format conversion with CSRZ-DPSK signal becomes a highly significant research topic. Wang and Sun demonstrated CSRZ-DPSK to RZ-DPSK format conversion by exploiting non-degenerate four-wave mixing (FWM) in a highly nonlinear fiber (HNLF).[15] Zhang and Yu demonstrated a format conversion scheme for multi-channel CSRZ-DPSK to NRZ-DPSK signals by utilizing a single delay interferometer (DI) with half bit delay.[16] So far, only a periodically poled lithium niobate (PPLN)-based scheme for NRZ/RZ-DPSK to CSRZ-DPSK conversion has been proposed and numerically demonstrated.[17] Unfortunately, the PPLN-based scheme uses the cascaded second-order nonlinearities, thus it has the disadvantage of low conversion efficiency and limiting in multi-channel conversion. Recently, format converters based on nonlinear polarization rotation (NPR) of SOA have become attractive due to their simple structure, higher ER and response speed. However, only NRZ-OOK/DPSK to RZ-OOK/DPSK and OOK to BPSK format conversions using NPR of SOA have been reported until now.[18−20] In this work, by NPR of SOA, we investigate an all-optical format conversion scheme capable of converting 4-channel NRZ/RZ-DPSK to CSRZ-DPSK signals simultaneously for the first time. The proposed scheme has the advantages of high conversion efficiency and simple structure.

The experimental setup is shown in Fig. 1. Four WDM channels (wavelength from $\lambda_1$ to $\lambda_4$) are combined by an array waveguide grating (AWG) and modulated via two Mach–Zehnder modulators (MZMs) where the first MZM converts the format to NRZ-DPSK and the second MZM converts it to RZ-DPSK format. The 4-channel lights are driven by the electrical data (PRBS $2^{31}$-1) from a pulse pattern generator (PPG) at 10 Gb/s. Meanwhile, a 10 GHz clock signal with sine curve at wavelength $\lambda_5$ is generated by MZM3 from the same PPG. An erbium-doped fiber amplifier (EDFA) is employed to set the desired clock signal power, and a tunable optical delay line (ODL) is used to synchronize the clock signal with the NRZ/RZ-DPSK signals. Then, the NRZ/RZ-DPSK signals are injected to SOA as probe signals due to the fact that their powers do not significantly affect the dynamics of the SOA. The clock signal with strong power is coupled into the SOA via the circulator as

*Supported by the National Natural Science Foundation of China under Grant Nos 61425022, 61522501, 61675004, 61307086, 61475024, 61672290, 61475094 and 61605013, the National Basic Research Program of China under Grant Nos 2015AA015501, 2015AA015502, 2015AA015504, 2015AA016904 and 2015AA016901, and the Beijing Nova Program under Grant No Z141101001814048.

**Corresponding author. Email: maoyy@nuist.edu.cn

© 2017 Chinese Physical Society and IOP Publishing Ltd

control signal. When the control signal couples to the SOA, the nonlinear polarization rotation occurs due to a phase shift difference between the transverse electric (TE) and transverse magnetic (TM) modes. Following the concept of principal state of polarization (PSP),[21] it has been reported that there exists a rotation axis on the Poincaré sphere (PS) with respect to the variation of SOA parameters.[22] The parameters mentioned here include bias current, control signal power, temperature and stress, etc. Due to the fact that the bias current is fixed, the temperature and stress vary slightly, the rotation axis is decided by the control signal power in our experiments. Using the proposed procedure in Ref. [22], a linear state of polarization (SOP) of the probe light can be generated and maintained during the course of the NPR induced by the control signal. Limited by the experimental condition, the fibers used in the experiment are single-mode fibers (SMFs), and provided that polarization maintaining fibers (PMFs) are used, the linear SOP of the output signal will be better maintained.

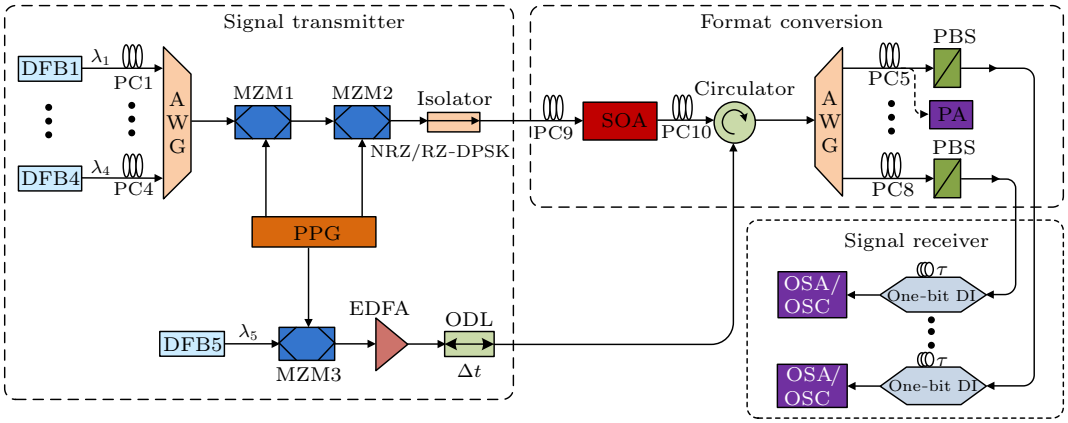


**Fig. 1.** Structure of the format converter based on nonlinear polarization rotation of SOA.

The system contains ten polarization controllers (PC). PCs 1–4 are used to adjust polarization of the input probe signal. PCs 9 and 10 are used to find the PSP. The polarization analyzer (PA) is used to monitor the SOP of the output signal, and then we replace the PA with a polarization beam splitter (PBS) after observing the NPR with linear polarization maintenance. PCs 5–8 are used to adjust the polarization of the amplified signals with the orientation of the PBSs, at first, PCs 5–8 are set in such a way that the probe beams cannot pass through the PBSs if only the probe beams are present. When the control beam is coupled into the SOA, the polarization of the probe signals is rotated. As a consequence, some probe light can pass through the PBSs, and an increase in the intensity of the control signal leads to an increase in the polarization rotation azimuth of the probe light. Thus the polarization rotation azimuth of different parts of probe signals varies due to the fact that the sine control signal is used. Thus by adjusting the polarizers which composed with PCs 5–8 and PBSs, the pulse widths of the converted signals can be finely tuned. In the case of NRZ-DPSK to CSRZ-DPSK conversion, to compress the probe signals, the transmission directions of the polarizers are set close to polarization direction with the higher power part of the probe signals. For the input probe signals being RZ-DPSK signals, the signal pulses can be broadened by adjusting the transmission directions of polarizers close to polarization direction with the lower power part of the probe signals, and thus the CSRZ-DPSK signal can be received. At signal receiver module, a one-bit delay interferometer (DI) is used to demodulate the signal, a spectrum analyzer (OSA) and an oscilloscope (OSC) are used to observe the spectrum and waveform, respectively.

In the experiment, the optical power level of each channel probe and control signals are −13 and 5 dBm, respectively. The wavelengths of the input probe signals span 3.2 nm, from 1546.52 nm to 1556.12 nm. The clock signal is located in the middle of the SOA bandwidth with 1551.34 nm. The SOA with 100 ps recovery time is biased at 200 mA.

Figure 2 shows the experimental results of NRZ-DPSK to CSRZ-DPSK format conversion. The measured spectra of the input probe signals and the converted signals are shown in Figs. 2(a) and 2(b). Figures 2(c) and 2(d) depict the detailed spectra of the input and the converted signals with 1556.12 nm wavelength. It can be seen that the optical carrier of the idler is suppressed, corresponding to the characteristic of CSRZ format. All the measured eye diagrams are presented in Figs. 2(e)–2(h). From top to bottom, the four lines show the 4-channel eye diagrams of the input NRZ-DPSK signals, the demodulated NRZ-DPSK signals, the converted CSRZ-DPSK signals and the demodulated CSRZ-DPSK signals, respectively. In the experiment, the NRZ-DPSK signals are generated by MZM, therefore, power dips appear in the NRZ-DPSK signals. However, these power dips do not result in distortion of the converted signals, as shown in Fig. 2(g). In addition, some chirp may be introduced

to the pulses by NPR inevitably, but the chirp does not deteriorate the receiver sensitivity of the demodulated CSRZ-DPSK signal as shown in Fig. 2(h). It is because the chirp is identical from pulse to pulse. All the clear and open eye diagrams of the converted and their demodulated signals demonstrate high quality format conversion performance.

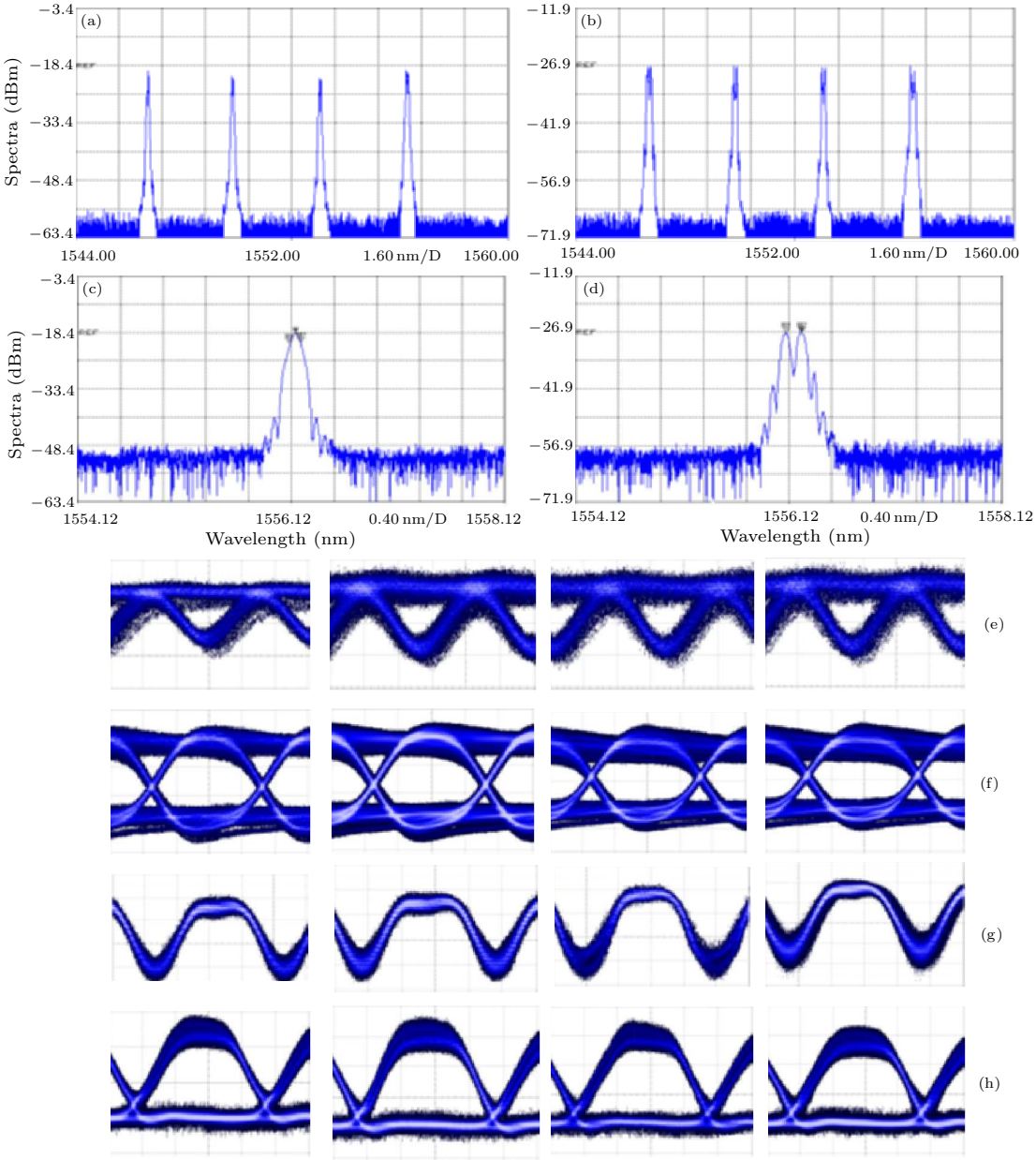


**Fig. 2.** Experimental results. Spectra of input NRZ-DPSK signals (a), converted CSRZ-DPSK signals (b), input 1556.12 nm NRZ-DPSK signal (c) and converted 1556.12 nm CSRZ-DPSK signal (d). Eye diagrams of the input 4-channel NRZ-DPSK and their demodulated signals ((e)–(f)) and the converted 4-channel CSRZ-DPSK and their demodulated signals ((g)–(h)).

Figure 3 shows the experimental results of RZ-DPSK to CSRZ-DPSK format conversion. In the experiment, the RZ-DPSK is with 50% duty cycle and the pulse duty cycle is defined as $T_{\mathrm{FWHM}}/T_{\mathrm{S}}$, where $T_{\mathrm{FWHM}}$ is the pulse width (full width at half-maximum intensity), and $T_{\mathrm{S}}$ represents the symbol duration. The measured spectra of the input probe signals and the converted signals are shown in Figs. 3(a) and 3(b). Figures 3(c) and 3(d) depict the detailed spectra of the input signal and the converted signal with 1556.12 nm wavelength. It can also be seen that the optical carrier of the idler is suppressed, corresponding to the characteristic of CSRZ format. All the measured 4-channel eye diagrams are presented in Figs. 3(e)–3(h). From top to bottom, the four lines show the eye diagrams of the input RZ-DPSK signals, the demodulated RZ-DPSK signals, the converted CSRZ-DPSK signals and the demodulated CSRZ-DPSK signals, respectively. Compared with Figs. 2(g) and 3(g), we can see that power jitter of the converted CSRZ-DPSK is more se-

rious for RZ-DPSK to CSRZ-DPSK conversion. This is due to the fact that in this type of conversion, to broaden the pulsewidth, the transmission directions of polarizers need to be set close to polarization direction with the lower power part of the probe signals, therefore, more optical power has been compressed, resulting in lower optical power output.

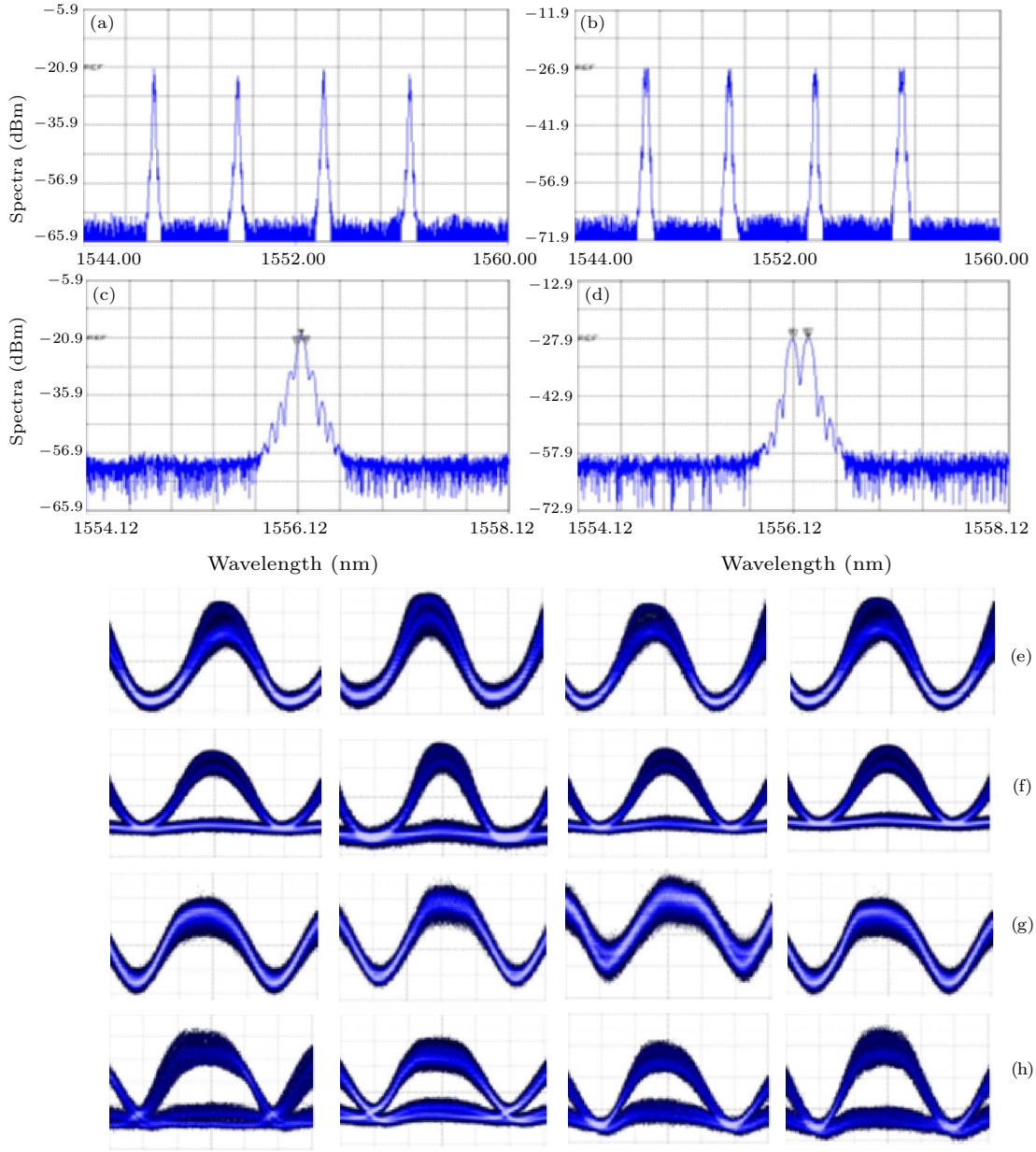


**Fig. 3.** Experimental results. Spectra of input RZ-DPSK signals (a), converted CSRZ-DPSK signals (b), input 1556.12 nm RZ-DPSK signal (c), and converted 1556.12 nm CSRZ-DPSK signal (d). Eye diagrams of the input 4-channel RZ-DPSK and their demodulated signals [(e)–(f)] and the converted 4-channel CSRZ-DPSK and their demodulated signals [(g)–(h)].

By comparing the above spectra, it can be obtained that NRZ/RZ-to-CSRZ format conversions are successfully implemented. Especially, the clear and open eye diagrams of the converted signal and its demodulated signal demonstrate high quality wavelength conversion performance. The converter has the potential to deploy more number of wavelengths in the whole C-band with higher control signal power and lower power of each probe signal. Since the power of each channel probe signal is much lower than that of the control signal, the nonlinear effects mainly occur between probe signals and the control signal. Subsequently, the crosstalk between probe signal channels is relatively weak even if the wavelength interval becomes smaller. Due to the limited optical source, 4-channel input probe signals (with 3.2 nm span) are simultaneously converted in our experiment.

Processed by a one-bit DI, the signals have been demodulated for evaluation. The bit error rate (BER) measurements are performed for all the channels. Fig-

ure 4(a) shows the BER results of the 4-channel original NRZ-DPSK and their converted CSRZ-DPSK signals. An average received power of −15.3 dBm per channel is required to achieve a BER of $10^{-9}$ for the NRZ-DPSK formats, whereas the converted formats require a lower power of −16.1 dBm to attain the same bit error rate. Figure 4(b) shows the BER results of RZ-DPSK and their converted CSRZ-DPSK signals. For the RZ-DPSK case, the received power required for $10^{-9}$ BER is −16.4 dBm, while for the converted format it is −15 dBm. Thus as compared with the original NRZ-DPSK and RZ-DPSK signals, the power penalties of the converted CSRZ-DPSK signals are −0.8 dB and 1.4 dB, respectively. The small power penalties indicate high quality system performance.

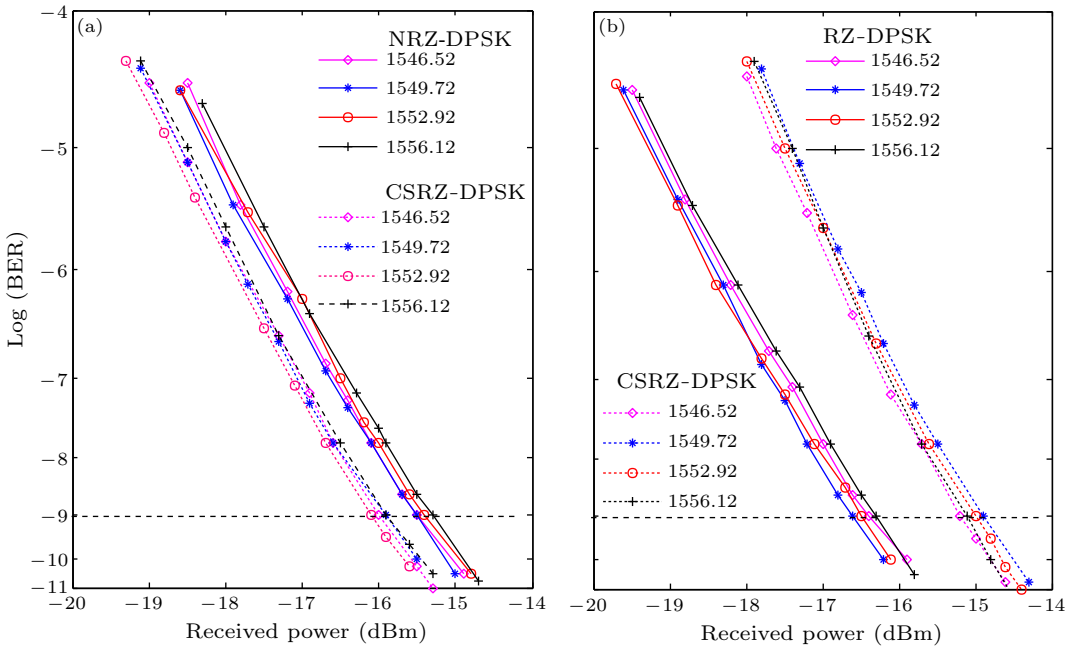


**Fig. 4.** BER characteristics for the 4-channel format conversion: (a) NRZ-DPSK to CSRZ-DPSK, and (b) RZ-DPSK to CSRZ-DPSK.

In summary, all-optical format conversion from NRZ/RZ-DPSK to CSRZ-DPSK based on SOA-NPR has been experimentally demonstrated. The 4-channel NRZ/RZ-DPSK signals at 10 Gb/s are shown to be converted to the corresponding CSRZ-DPSK signals simultaneously. For all the cases of probe NRZ/RZ-DPSK wavelengths, the converted signals experience small average penalties of −0.8/1.4 dB at BER of $10^{-9}$, compared with the original signal. In addition, the optical spectra and the open eye diagrams of the converted signal show high quality wavelength performance. It is, therefore, recommended to deploy the proposed scheme in WDM networks.

## References

[1] Willner A E, Khaleghi S, Chitgarha M R and Yilmaz O F 2014 *J. Lightwave Technol.* **32** 660
[2] Hui Z Q, Zhang B and Zhang J G 2016 *J. Mod. Opt.* **63** 724
[3] Fu S, Zhong W, Shum P and Wen Y 2009 *Opt. Commun.* **282** 2143
[4] Yu Y, Zhang X and Huang D 2007 *Opt. Express* **15** 5693
[5] Dong J, Zhang X, Xu J, Huang D and Fu S 2007 *Opt. Express* **15** 2907
[6] Wang L, Dai Y and Lei H 2011 *IEEE Photon. Technol. Lett.* **23** 368
[7] Zou B, Yu Y, Wu W and Zhang X 2012 *IEEE Photon. Technol. Lett.* **24** 1091
[8] Pan Y, Yan L and Yi A 2016 *Opt. Lett.* **41** 1620
[9] Tabares A, Victor P and Josep P 2017 *Optical Fiber Communication Conference* p Th1K.3
[10] Yu Y, Zou B, Wu W and Zhang X 2011 *Opt. Express* **19** 14720
[11] Sharif G M, Nguyen-the Q and Matsuura M 2014 *IEICE Trans. Electron.* **E97. C** 755
[12] Chattopadhyay T 2010 *Appl. Opt.* **49** 5226
[13] Lize Y K and Wu X 2008 *Opt. Express* **16** 4228
[14] Yao S, Fu S and Wang H 2014 *J. Opt. Commun. Networking* **6** 355
[15] Wang J and Sun J 2009 *Opt. Express* **17** 12555
[16] Zhang Z and Yu Y 2011 *Opt. Express* **19** 12427
[17] Wang J and Sun J 2008 *IEEE Photon. Technol. Lett.* **20** 1039
[18] Yang X, Mishra A K and Manning R J 2007 *Electron. Lett.* **43** 469
[19] Mao Y, Sheng X and Wu C 2015 *Appl. Opt.* **54** 8130
[20] Jiang H, Wen H and Han L 2007 *IEEE Photon. Technol. Lett.* **19** 1985
[21] Poole C D and Wagner R E 1986 *Electron. Lett.* **22** 1029
[22] Fu S, Zhong W, Shum P, Wu C and Zhou J 2007 *IEEE Photon. Technol. Lett.* **19** 1931